

Fig. 22A-3-001. TlGaSe₂. $\kappa'_{[100]}$, $\kappa'_{[010]}$, $\kappa'_{[001]}$ vs. T [88Hoc].

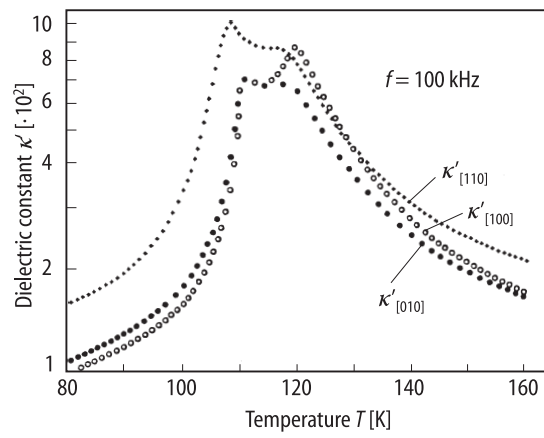


Fig. 22A-3-002. TlGaSe₂. $\kappa'_{[100]}$, $\kappa'_{[010]}$, $\kappa'_{[110]}$ vs. T [88Hoc].

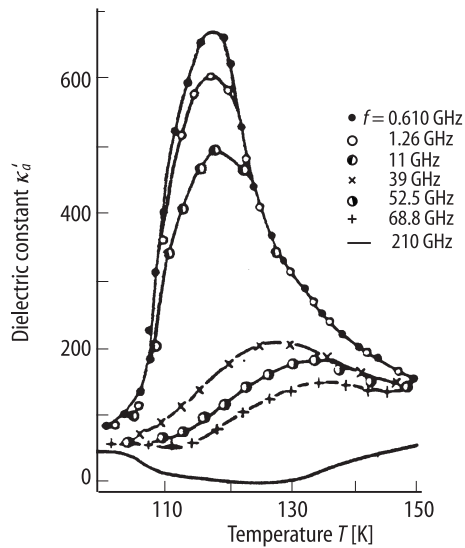


Fig. 22A-3-003. TlGaSe₂. κ'_d vs. T [87Ban]. Parameter: f .

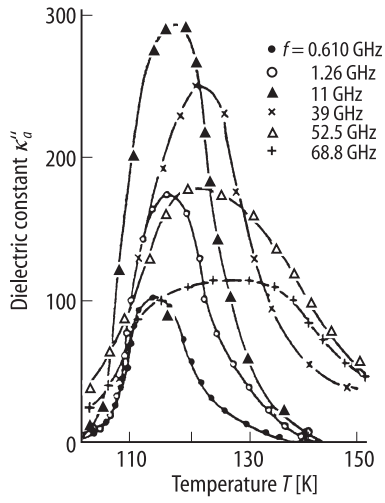


Fig. 22A-3-004. TlGaSe₂. κ'_a vs. T [87Ban]. Parameter: f .

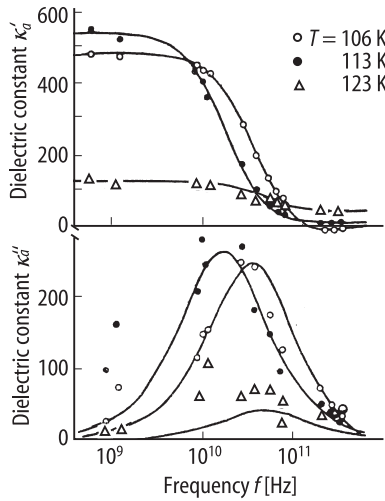


Fig. 22A-3-005. TlGaSe₂. κ'_a , κ''_a vs. f [87Ban]. Parameter: T .

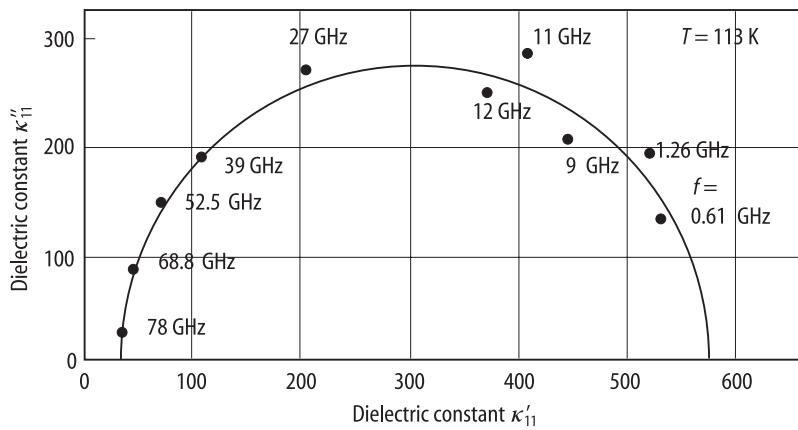
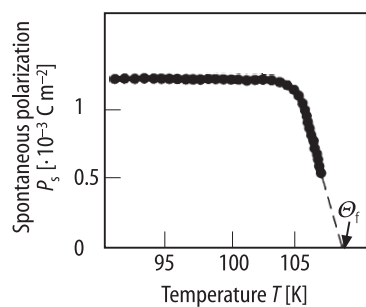
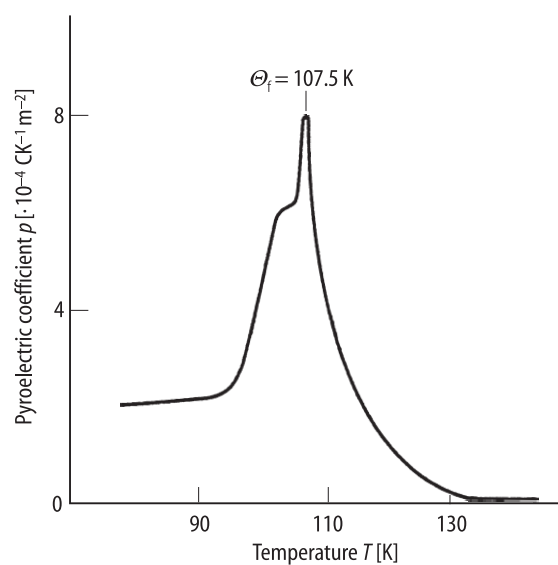


Fig. 22A-3-006. TlGaSe₂. Cole-Cole diagram of complex dielectric constant at 113 K [87Ban].

**Fig. 22A-3-007.** TlGaSe₂. P_s vs. T [91Sar].**Fig. 22A-3-008.** TlGaSe₂. p vs. T [91Sar]. p : pyroelectric coefficient.

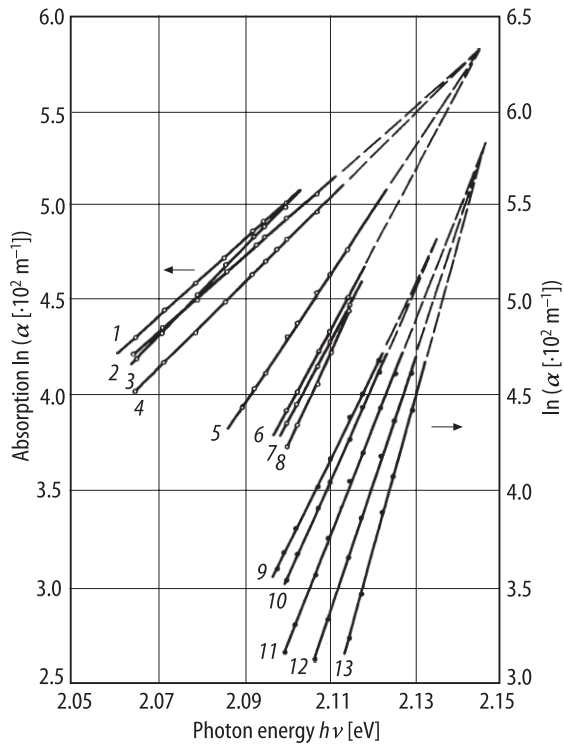


Fig. 22A-3-009. TlGaSe_2 . $\ln\alpha$ vs. $h\nu$ [86All]. α : absorption coefficient in units of 10^2 m^{-1} . $E \perp \sigma$ (symmetry plane). Parameter: T . Curve 1: 258 K, 2: 294 K, 3: 240.5 K, 4: 186 K, 5: 151 K, 6: 123.5 K, 7: 118 K, 8: 113 K, 9: 106 K, 10: 103.5 K, 11: 94.5 K, 12: 78 K, 13: 59 K.

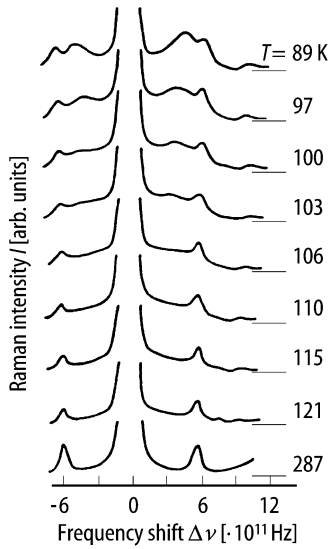


Fig. 22A-3-010. TlGaSe_2 . I vs. $\Delta\nu$ [88Kul]. I : Raman scattering intensity of the $Y(XX)Z$ geometry. Parameter: T .

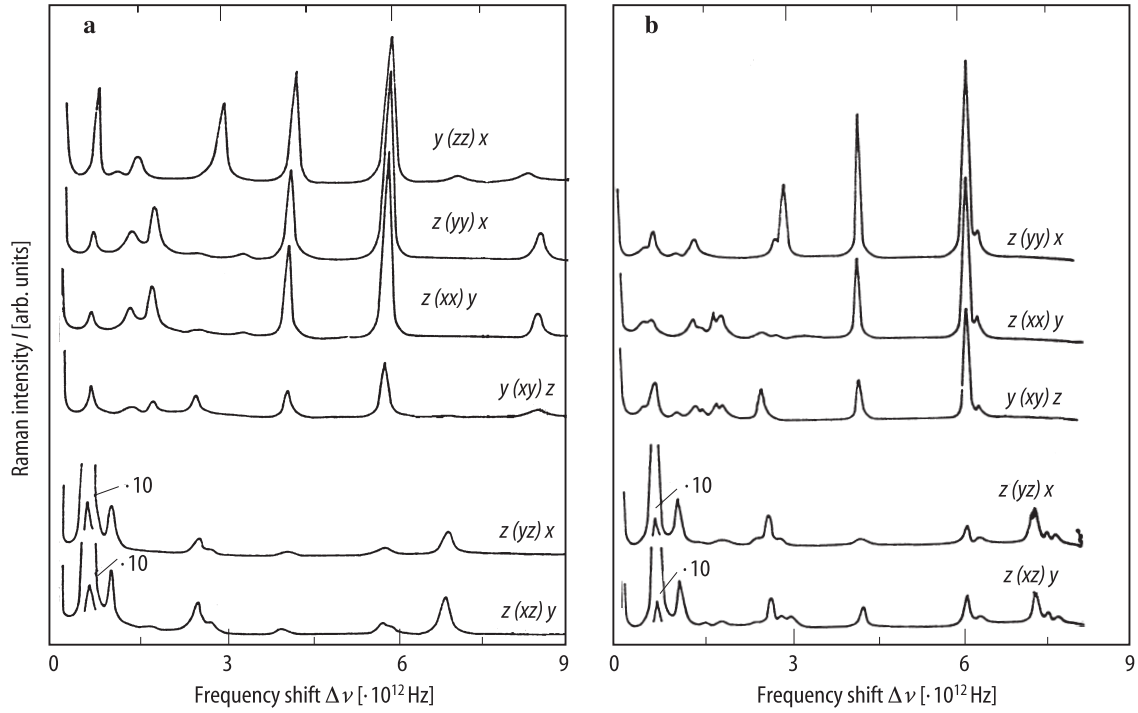


Fig. 22A-3-011. TlGaSe₂. I vs. $\Delta\nu$ [89Dur1]. I : Raman scattering intensity at (a) 287 K and (b) 90 K. Parameter: scattering geometry.

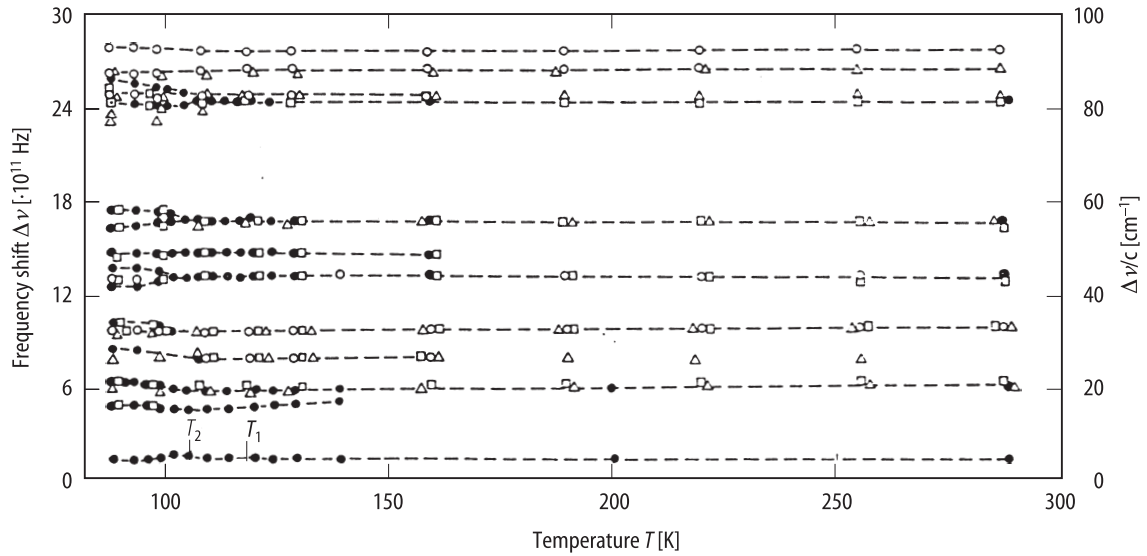


Fig. 22A-3-012. TlGaSe₂. $\Delta\nu$ vs. T [89Dur1]. $\Delta\nu$: Raman scattering frequency shift of $Y(XX)Z$ (full circle), $Y(ZZ)X$ (open circle), $Y(XY)Z$ (square) and $Z(XZ)Y$ (triangle) geometries. $T_1 = 120$ K, the unit cell quadruples in c -direction. $T_2 = (107 \pm 2)$ K, the soft mode frequency becomes zero.

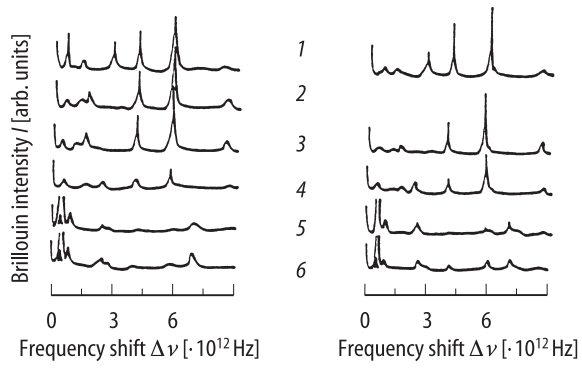


Fig. 22A-3-013. TlGaSe₂. I vs. $\Delta\nu$ [89Dur2]. I : Brillouin scattering intensity of the LA mode.

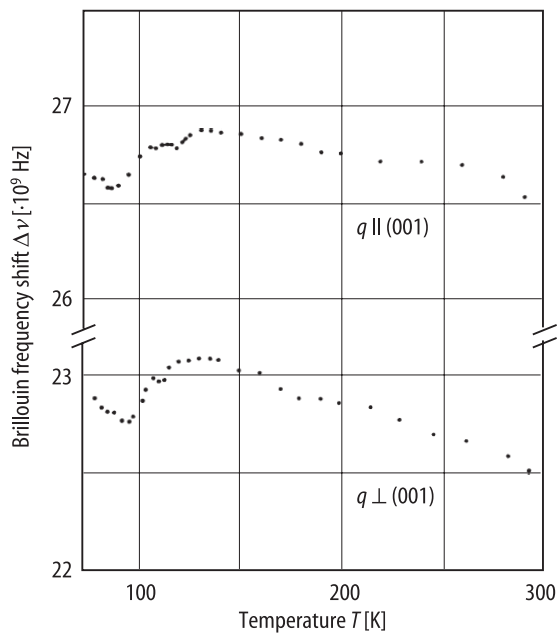


Fig. 22A-3-014. TlGaSe₂. $\Delta\nu$ vs. T [88Lai]. $\Delta\nu$: Brillouin scattering frequency shift. Parameter: directions of q .